Exciton diffusion in CdSe

J. Erland, B. S. Razbirin,* K.-H. Pantke, V. G. Lyssenko,† and J. M. Hvam
Fysisk Institut, Odense Universitet, Campusvej 55, DK-5230 Odense M, Denmark
(Received 8 September 1992)

In transient laser-induced grating experiments, the diffusion coefficients and lifetimes of free excitons are determined in CdSe at temperatures between 2 and 40 K and for different densities. We find that the diffusion coefficient D decreases and that the recombination lifetime T_1 increases with increasing temperature. The increase of T_1 with temperature is due to the release of excitons bound to impurities and to an increase of the radiative lifetime. From the measured D values for motion parallel and perpendicular to the crystal c axis, we extract momentum relaxation rates which are discussed in terms of exciton-acoustic-phonon scattering. In pure samples, and for lattice temperatures $T < 10$ K, the interaction via the deformation potential is dominating, while for higher temperatures, the interaction via the piezoelectric potential becomes significant.

I. INTRODUCTION

Excitons, or bound states of electron-hole pairs, are the lowest elementary electronic excitations in semiconductors at low temperature, and are typically created by an optical excitation either resonantly or in the band continuum. Being neutral particles, their spatial redistribution does not carry any current, but is nevertheless very important for energy transport and relaxation in semiconductors.

Since excitons, even at relatively low densities, alter the optical parameters (absorption coefficient and refractive index) near the exciton resonances, they can be monitored by nonlinear optical spectroscopies like, e.g., four-wave mixing. In particular, degenerate four-wave mixing (DFWM) in a three-beam configuration with picosecond time resolution, or transient laser-induced gratings (TLIG), have proven very powerful in determining both the diffusion coefficient and the lifetime of photoexcited carriers, independently.[1,2] It is a contact-free and nondestructive technique, that recently has been used extensively to study exciton diffusion in pure elemental or binary compound semiconductors,[3] in systems where the excitons are confined by nanostructures (quantum wells, wires, and dots),[4] and in systems where fluctuating potentials from interface roughness or alloy disorder tend to localize the excitons.[5] In the present paper, we will concentrate on the first item, presenting a more rigorous study of diffusion in CdSe than previously reported.[6] We present a detailed investigation of the temperature dependence of the anisotropic diffusion coefficient of excitons at low temperatures, and simultaneously we determine the recombination lifetime T_1 of excitons. We will discuss the different scattering mechanisms in the semiconductor that are responsible for the magnitude and the temperature dependence of the momentum relaxation times and thereby the diffusion coefficient.

The paper is organized as follows: In Sec. II we give a brief introduction to the scattering and diffusion of excitons. The basic ideas of the experimental method are explained in Sec. III. After some notes about the experimental setup in Sec. IV, we present and discuss our results in Sec. V.

II. SCATTERING AND DIFFUSION OF EXCITONS

In a classical approach, the diffusion coefficient D is connected to the momentum relaxation time τ_p of excitons by the relation

$$D=\frac{k_B T}{m^*}\tau_p \ , \quad t \gg \tau_p \ , \tag{1}$$

where $m^*=m_e+m_h$ is the total exciton effective mass, m_e and m_h are the effective electron and hole masses, k_B is the Boltzmann constant, and T is the (effective) temperature of the exciton gas. We indicate that Eq. (1) is only valid for times t much larger than the momentum relaxation time. In the limit $t \approx \tau_p$ the problem is governed by ballistic transport, which is not treated here.

The exciton momentum is changed by the interaction with other particles and quasiparticles such as impurities and phonons, and we assume that τ_p can be described by the sum of all scattering rates Γ_i.

$$\frac{1}{\tau_p}=\sum_i \Gamma_i \ . \tag{2}$$

We neglect exciton-exciton scattering, which is only of importance for high-excitation density, and the scattering with optical phonons which gives no significant contribution for $T < 50$ K.[7] In the following, we discuss the interaction with acoustic phonons giving rise to a characteristic temperature dependence of the scattering rates, which enter into the calculation of the exciton diffusion coefficient.

The scattering of excitons in CdSe with acoustic phonons has two contributions, due to the interaction via the deformation potential and via the piezoelectric potential. The deformation potential gives rise to a short-ranged scattering center with scattering rate Γ_{dp}:[8,9]

$$\Gamma_{dp}=\frac{\sqrt{2}(D_c-D_v)^2 k_B T(m^*)^{3/2}E^{1/2}}{\pi\rho v^2\hbar^4}\ , \tag{3}$$

where D_c-D_v is the deformation potential, ρ is the mass density of the crystal, v is the longitudinal sound velocity, and E is the kinetic energy of the exciton. Approximating the kinetic energy by the thermal average value, the temperature and mass dependence of the momentum relaxation rates via the deformation potential is given by

$$\Gamma_{dp}\propto(m^*T)^{3/2}\ . \tag{4a}$$

In anisotropic crystals, the excitons can furthermore scatter via the long-ranged piezoelectric potential. Piezoelectric scattering is highly anisotropic, i.e., it depends strongly on the wave vectors of the involved particles and is strongest parallel to the c axis. In the limit of phonon wave vectors comparable to (or larger than) the inverse exciton radius, the piezoelectric interaction gives rise to another temperature and mass dependence of the scattering rate Γ_{pe}:[9]

$$\Gamma_{pe}\propto(m^*T)^{1/2}\ . \tag{4b}$$

By measuring the temperature dependence of the diffusion coefficient, we discuss the different interactions responsible for the momentum relaxation rates.

III. THE TRANSIENT GRATING METHOD

This technique, which is based on a time-resolved three-beam DFWM, has been developed during the last decade into a very useful spectroscopic technique.[10,11] Time-resolved coherent DFWM yields information about coherence and phase relaxation of the optical resonances (excitons) involved.[12] In this work, however, we merely focus on the light-induced incoherent density grating excited resonantly in the lowest exciton (A) resonances in CdSe.

Consider two laser beams incident on the surface of the crystal with a small mutual angle Θ, as sketched in the inset of Fig. 1. The interference pattern between the two incident beams produces a grating, which has two contributions: A field grating due to the coherent interaction of the two incident beams with the sample, and a real-density grating due to the resonant excitation. The first contribution is only significant on a time scale limited by the phase relaxation time of the excitations in the crystal. The high-diffraction efficiency of this coherent grating experienced by a third delayed beam[12] is not investigated further in this work. On a time scale beyond the phase relaxation time, the second contribution is significant. The density grating created, proportional to the intensity of the two incident interfering light fields, is a harmonic grating with a modulation $\Delta N(t)$ of the density of excitons $N(t)$ given by

$$\Delta N(t)=\frac{N(t)}{2}\exp(-\alpha z)\cdot\{(1+\cos(2\pi x/\Lambda)\}\ , \tag{5}$$

where α is the absorption coefficient, x is the direction of diffusion, z is the depth in the crystal, and Λ is the grating constant:

$$\Lambda=\frac{\lambda}{2\sin\left[\frac{\Theta}{2}\right]}\ , \tag{6}$$

where λ is the wavelength of the exciting laser. If only recombination and diffusion of excitons contribute to the decay of the transient grating, the decay is governed by

$$\frac{\partial\Delta N}{\partial t}=D\cdot\nabla(\Delta N)-\frac{\Delta N}{T_1}\ , \tag{7}$$

where we assume the diffusion coefficient D to be independent of space coordinates. Inserting Eq. (5) into Eq. (7) we find the decay time T_D of the intensity of the first diffracted order $I\propto[\Delta N(t)]^2$ as[13]

$$\frac{1}{T_D}=\frac{2}{T_1}+\frac{8\pi^2 D}{\Lambda^2}\ . \tag{8}$$

By measuring the decay time T_D as a function of the grating constant Λ, we determine the diffusion coefficient D from the slope of T_D^{-1} versus $1/\Lambda^2$. By extrapolation to $1/\Lambda^2=0$, we also determine the recombination lifetime T_1 of the excitons.

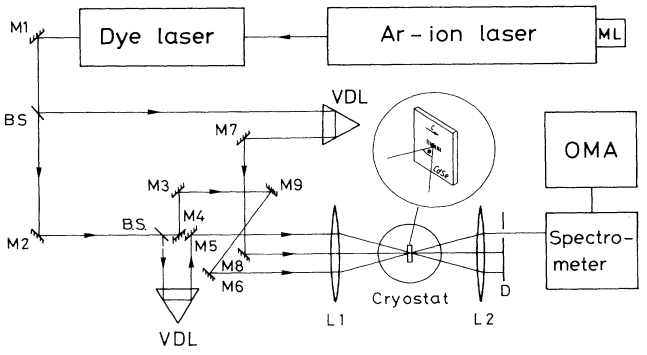

FIG. 1. Schematic diagram of the experimental setup. B.S.: beam splitter; D: diaphragm; $L1$ and $L2$: lenses; $M1$–$M9$: mirrors; ML: mode locker; OMA: optical multichannel analyzer; VDL: variable delay line.

IV. EXPERIMENTAL SETUP

Measurements in the temperature range of 2–40 K are realized in the experimental setup sketched in Fig. 1. We investigate CdSe samples of good optical quality, as grown from the vapor phase with the c axis in the plane of the platelets, about 10 μm thick. They are immersed in a variable-temperature helium cryostat. Pulses of about 7 ps [full width at half maximum (FWHM)] and 82-MHz repetition rate are generated by a mode-locked argon-ion laser which pumps synchronously a tunable dye laser (DCM). The generated pulses have a spectral width of 2.4 meV and all measurements are performed with a linear polarization perpendicular to the c axis, $E\perp c$. The laser beam is split into three separate contributions which are spatially overlapping in the focus on the crystal surface. Two of the beams are temporally overlapping and they produce the transient grating, which is probed by the third delayed beam. The first-order

diffraction of this delayed beam is dispersed in a spectrometer, which has a resolution of 0.2 meV, and is detected, time integrated, by an optical multichannel analyzer (OMA) system. The spectra are recorded as a function of the delay τ of the third beam. Due to the anisotropy of the hexagonal CdSe crystals, different diffusion coefficients $D_{\|c}$ and $D_{\perp c}$ are expected parallel and perpendicular to the c axis, respectively. By a simple rotation of the crystal, a grating can be created parallel or perpendicular to the c axis, and the anisotropy of the diffusion can be measured.

V. RESULTS AND DISCUSSION

We obtain decay curves as shown in Figs. 2 and 3 for temperatures $T=12$ and 25 K, when exciting with an excitation density of about 30 kW/cm^2 in the spectral range just below the $A_{n=1}$ exciton. These curves, which are measured for a grating vector **G** parallel to the c axis (**G**$\|c$), consist of three parts: A spike around $\tau=0$, due to the coherent interaction between the polarization of the crystal and the probe beam; a subsequent nonexponential decay, due to the thermalization of excitons; and a final exponential decay for $\tau>600$ ps governed only by diffusion and recombination of excitons, which are in quasiequilibrium with the lattice. The initial part for $\tau<600$ ps strongly depends on the temperature and on the kinetic excess energy of the excitons. The slopes, especially for large grating constants, diminish with rising temperature. Increasing the temperature further to 30 K, these curves even reveal a small maximum of intensity around $\tau=200$ ps.

Generating the excitons near the $A_{n=2}$ exciton resonance with an excess energy of about 10 meV causes a steeper initial decay, which after 500 ps bends over to the shape of the decay curves measured near the $A_{n=1}$ resonance, as shown in Fig. 4. We attribute the initial decay to the cooling of the excitons toward the final thermalized distribution, which does not depend much on the excitation conditions. This cooling is known to take place on a time scale of about 500 ps.[14] On this time scale, a contribution to the initial decay from high-excitation effects, i.e., biexciton formation and exciton-exciton scattering, is present.[6] We will in the following concentrate on the decay for $\tau>600$ ps, where the excitons are in quasiequilibrium with the lattice and Eq. (8) can be applied to determine the diffusion coefficient and the lifetime of the particles. The insets of Figs. 2–4 demonstrate the linear dependence between T_D^{-1} and $1/\Lambda^2$.

The resulting recombination lifetime T_1 is shown in Fig. 5 as a function of temperature increasing from $T_1=2$ ns at 2 K to $T_1=6$ ns at 40 K. We tentatively explain the increase of the recombination lifetime with temperature by thermal release of impurity-bound excitons[15,16] and by an increase of the radiative lifetime of free excitons. In II-VI materials, the radiative lifetime is

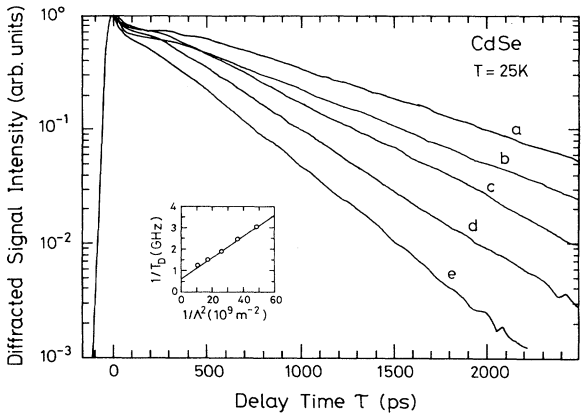

FIG. 3. Diffracted signal intensity for excitation ($\approx$30 kW/cm^2) just below the $A_{n=1}$ exciton resonance for a lattice temperature of $T=25$ K vs delay τ for different grating constants: (a) $\Lambda=7.6$ μm, (b) $\Lambda=6.3$ μm, (c) $\Lambda=5.4$ μm, (d) $\Lambda=4.7$ μm, and (e) $\Lambda=4.1$ μm, with grating vector **G**$\|c$.

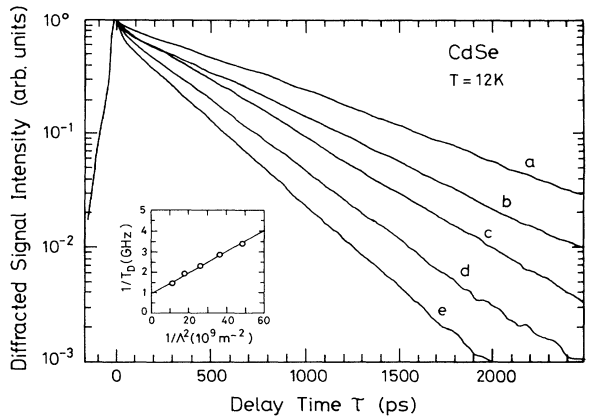

FIG. 2. Diffracted signal intensity for excitation ($\approx$30 kW/cm^2) just below the $A_{n=1}$ exciton resonance for a lattice temperature of $T=12$ K vs delay τ for different grating constants: (a) $\Lambda=7.6$ μm, (b) $\Lambda=6.3$ μm, (c) $\Lambda=5.4$ μm, (d) $\Lambda=4.7$ μm, and (e) $\Lambda=4.1$ μm, with grating vector **G**$\|c$. The inset demonstrates the determination of D and T_1.

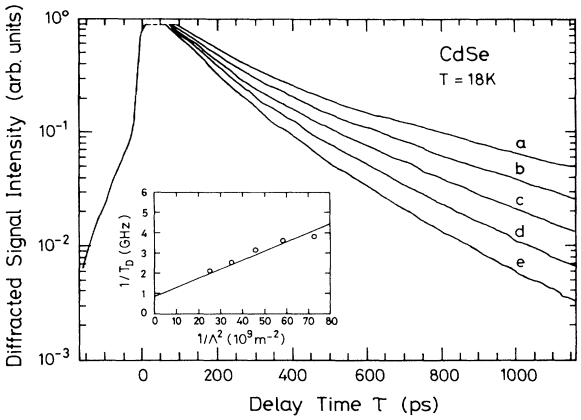

FIG. 4. Diffracted signal intensity for excitation ($\approx$30 kW/cm^2) just below the $A_{n=2}$ exciton resonance for a lattice temperature of $T=18$ K vs delay τ for different grating constants: (a) $\Lambda=6.3$ μm, (b) $\Lambda=5.4$ μm, (c) $\Lambda=4.7$ μm, (d) $\Lambda=4.1$ μm, and (e) $\Lambda=3.7$ μm, with grating vector **G**$\|c$.

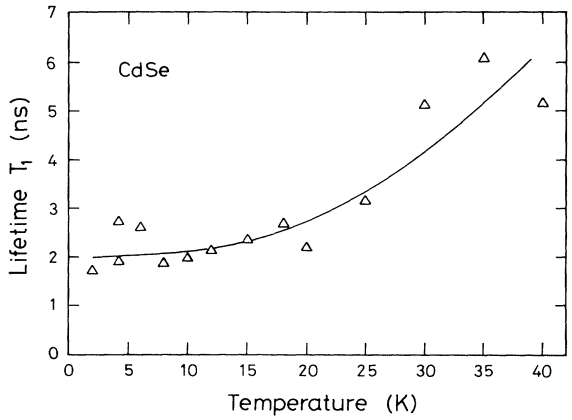

FIG. 5. Lifetime T_1 for the $A_{n=1}$ exciton vs temperature. The solid curve is only to guide the eye.

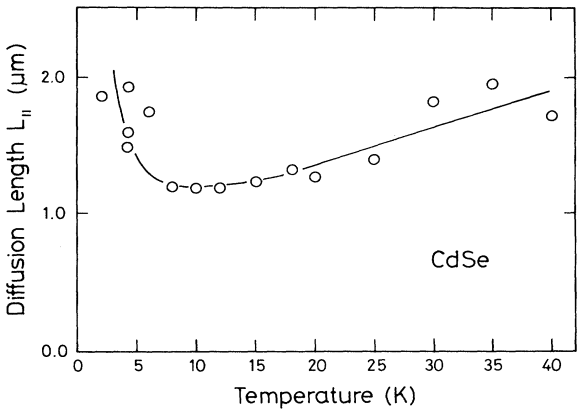

FIG. 7. Diffusion length $L_{\|}$ of excitons vs temperature. The solid curve is only to guide the eye.

of the same order of magnitude as the measured lifetimes,[17] and increases with increasing temperature due to the thermal occupation of states with large k vectors. We cannot in our measurements distinguish between the two contributions to the observed increase of the recombination lifetime.

The temperature dependence of the diffusion coefficient parallel $D_{\|c}$ and perpendicular $D_{\perp c}$ to the c axis is shown in Fig. 6. The diffusion coefficient decreases from $D_{\|c}=20$ cm^2/s at 2 K to $D_{\|c}=6.6$ cm^2/s at 12 K and stays nearly constant up to 40 K. The diffusion coefficient $D_{\perp c}$ is much larger ranging from $D_{\perp c}=140$ cm^2/s at 2 K decreasing to $D_{\perp c}=26$ cm^2/s at 30 K. The size of the circles in Fig. 4 indicates the standard deviation of the diffusion coefficient, when calculated from the $1/T_1$ versus $1/\Lambda^2$ plots (insets, Figs. 2–4). The experimental error is not included, but can be estimated from the reproducibility of the three points measured at 4.2 K to be about 15%. The inset of Fig. 6 shows the measured ratio between $D_{\perp c}/D_{\|c}$, which is decreasing with increasing temperature.

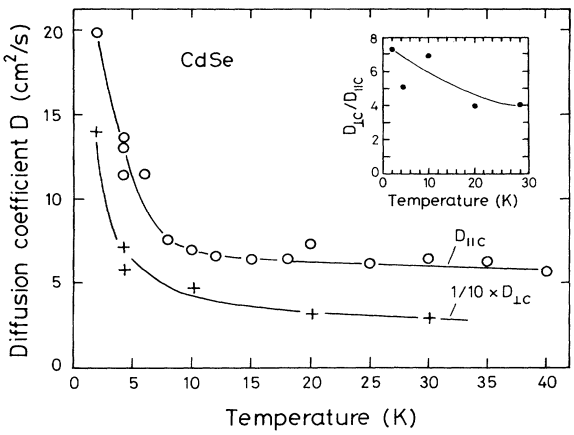

FIG. 6. Measured diffusion coefficient parallel $D_{\|c}$ and perpendicular $D_{\perp c}$ to the c axis. The solid curves are only to guide the eye. The inset shows the ratio $D_{\perp c}/D_{\|c}$.

The exciton diffusion length $L=\sqrt{DT_1}$ is plotted in Fig. 7 as a function of temperature. L decreases for low temperatures due to the decrease of D and shows a minimum around 10 K. The increase of the diffusion length for $T>10$ K is due to the increase of the lifetime.

Taking the relevant exciton masses of $m_{\perp}^{*}=0.40m_0$ and $m_{\|}^{*}=1.3m_0$,[18] and assuming that the exciton temperature coincides with the lattice temperature, we can from Eq. (1) calculate the momentum relaxation times τ_p. The largest momentum relaxation times at 2 K are $\tau_{p\perp}=280$ ps and $\tau_{p\|}=85$ ps, which demonstrate that we have satisfied the condition $t\gg\tau_p$ in Eq. (1).

It is evident that the corresponding momentum relaxation rates $1/\tau_p$ in Fig. 8 for diffusion perpendicular to the c axis increase as $T^{3/2}$ indicating deformation-potential scattering [Eq. (4a)] in the temperature range from 2 to

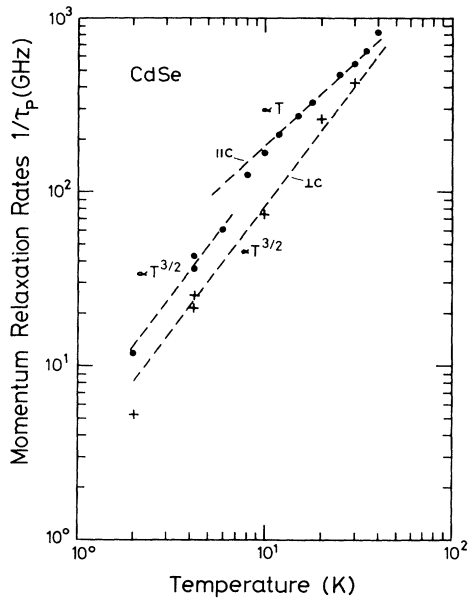

FIG. 8. Momentum relaxation rates parallel $1/\tau_{p\|c}$ (dots) and perpendicular $1/\tau_{p\perp c}$ (crosses) to the c axis for $m_{\|c}^{*}=1.3m_0$ and $m_{\perp c}^{*}=0.40m_0$.

30 K. This is also seen for diffusion parallel to the c axis for temperatures $T<8$ K. However, for $T>10$ K we find that the momentum relaxation rates are proportional to the temperature. For temperatures $8<T<10$ K, a steeper increase is observed and we suggest that both piezoelectric-potential and deformation-potential scattering are responsible for the observed temperature dependence above 10 K.

From Eqs. (1) and (4a), and by assuming isotropic deformation potentials and sound velocities, it can be seen that for deformation-potential interaction we have $D_{\perp c}/D_{\parallel c} \propto (m^*_{\parallel c}/m^*_{\perp c})^{5/2}$, while a smaller mass dependence is expected for piezoelectric potential interaction. The measured decrease of the ratio $D_{\perp c}/D_{\parallel c}$ with temperature in the inset of Fig. 6, from 7.3 at low temperatures to a value of 4.0 at higher temperatures, can be understood by the increase of piezoelectric scattering with temperature. For low temperatures, the ratio is mainly governed by interaction of excitons via the deformation potential, while for higher temperatures piezoelectric scattering becomes more significant. Assuming only deformation-potential interaction, the measured ratio of $D_{\perp c}/D_{\parallel c}=7.3$ gives a mass ratio of $m^*_{\parallel c}/m^*_{\perp c}=1.9$, which is smaller than the literature value of 3.2. We suggest that the observed discrepancy has several causes. If the laser-induced grating is not created strictly parallel or perpendicular to the c axis, a misalignment of a few degrees will reduce the measured ratio $D_{\perp c}/D_{\parallel c}$. Furthermore, we have neglected the anisotropy of the deformation potential and of the sound velocity in our considerations. Finally, contributions of other scattering mechanisms than deformation-potential interaction can decrease the ratio.

The temperature dependence of the scattering rates in Fig. 8 shows that exciton interaction with acoustic phonons is governing the diffusion in the investigated sample. However, from the temperature dependence of the recombination lifetime T_1 we concluded that trapping by impurities are limiting the lifetime of excitons at least at the lowest temperatures. We also investigate the influence of impurities on the scattering rates by measuring the intensity dependence of the diffusion coefficient, and observe a small increase of the measured diffusion coefficient with the excitation density, as shown in Fig. 9. This we attribute to the saturation of the impurities which otherwise contribute to scattering (momentum relaxation) as well as to recombination.[16] The measured increase of lifetime with intensity, shown in the inset of Fig. 9, supports this explanation. Thermal heating as well as exciton-exciton collisions at high intensity would increase the scattering rates and decrease the diffusion coefficient. Neglecting the latter, we can estimate a low-temperature impurity trapping rate of $\Gamma_{\text{imp}}=3$ GHz from the difference in magnitude of the diffusion coefficient of D for high and low intensities.

Impurity scattering or trapping may strongly change the value and the temperature dependence of the diffusion coefficient D. In Fig. 10, we have plotted measurements published previously by our group (crossed squares),[6] showing a slight increase of D with increasing temperature. They should be compared with the present

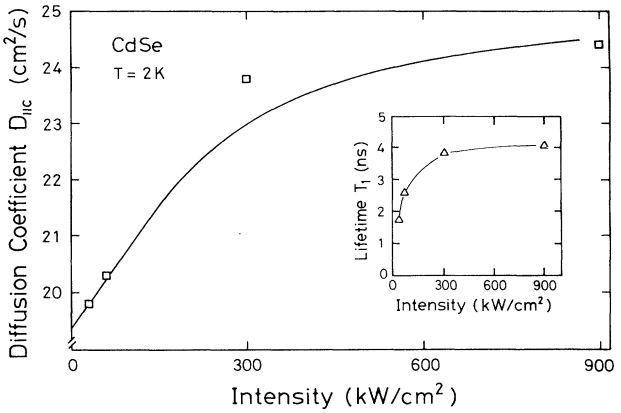

FIG. 9. Diffusion coefficient $D_{\parallel c}$ and lifetime vs excitation density. The solid curves are only to guide the eye.

results (solid squares), showing much larger values for D, but decreasing with increasing temperature. Equations (1) and (4) prove that an increase of D with increasing temperature cannot be explained by exciton-phonon scattering. To explain our former results, an additional scattering mechanism Γ_{imp}, diminishing the diffusion, has to be considered. The solid curves in Fig. 10 are diffusion coefficients calculated from Eqs. (1) and (3) with $1/\tau_p=\Gamma_{\text{dp}}(T)+\Gamma_{\text{imp}}$, assuming temperature- and k-vector-independent scattering (trapping) rates Γ_{imp}. For the longitudinal sound velocity v and the mass $m^*_{\parallel}=1.3$ m_0, we choose the literature values, but for the value of the deformation potential we take $D_c-D_v=6.3$ meV.[18,19] It can be seen that, with increasing impurity scattering rates, the diffusion coefficient decreases for very low temperature and decreases less pronouncedly for higher temperatures, leading to a maximum of the curve that depends on the impurity scattering rate. It should be mentioned that we describe the influence of impurity scattering more qualitatively than quantitatively, because we assume a temperature- and k-vector-independent exciton-impurity scattering term, neglect the interaction with

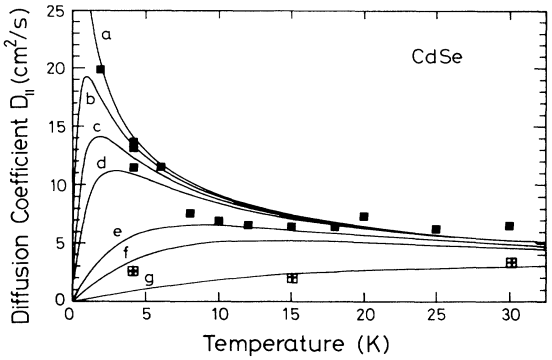

FIG. 10. Calculated diffusion coefficient D (see text) due to deformation-potential interaction and for different impurity scattering rates: (a) $\Gamma_{\text{im}}=0$, (b) $\Gamma_{\text{im}}=2$ GHz, (c) $\Gamma_{\text{im}}=5$ GHz, (d) $\Gamma_{\text{im}}=10$ GHz, (e) $\Gamma_{\text{im}}=50$ GHz, (f) $\Gamma_{\text{im}}=100$ GHz, (g) $\Gamma_{\text{im}}=500$ GHz. Solid squares are measured from Fig. 6 and crossed squares are measurements from Ref. 6.

phonons via the piezoelectric potential, and introduce a somewhat higher value for the deformation potential than found in the literature.[19] However, the slight increase of D with increasing temperature observed in Ref. 6 is evidence for high exciton-impurity scattering rates.

In conclusion, the measured recombination lifetimes of free excitons in the nanosecond range are increasing with increasing temperature because of release of impurity-bound excitons and because of an increase of the radiative lifetime. In pure samples, the measured diffusion coefficients D decrease with increasing temperature T. For deep temperatures we extract momentum relaxation rates $\tau_p \propto T^{2/3}$, due to the scattering with acoustic phonons via the deformation potential. For temperatures $T > 10$ K piezoelectric scattering becomes significant, at least for diffusion parallel to the c axis. In samples of less quality, an increase of D with increasing temperature can be observed.

ACKNOWLEDGMENT

The work was supported by the Danish Natural Science Research Council.

*Permanent address: A.F. Ioffe Physical-Technical Institute, 194021 St. Petersburg, Politekhnicheskaya 26, Russia.

†Permanent address: Institute of Microelectronics Technology and Superpure Materials, Chernogolovka, Moscow District, 142432, Russia.

[1]K. Jarašiūnas and H. J. Gerritsen, Appl. Phys. Lett. **33**, 190 (1978).

[2]I. Rückmann, K. Jarašiūnas, and E. Gaubas, Phys. Status Solidi B **128**, 627 (1985).

[3]Y. Aoyagi, Y. Segawa, and S. Namba, IEEE J. Quantum Electron. **QE-22**, 1320 (1986).

[4]D. Oberhauser, K.-H. Pantke, J. M. Hvam, G. Wiemann, and C. Klingshirn (unpublished).

[5]H. Schwab, K.-H. Pantke, J. M. Hvam, and C. Klingshirn, Phys. Rev. B **46**, 7528 (1992).

[6]K.-H. Pantke, J. Nørgaard, J. Erland, and J. M. Hvam, J. Lumin. **53**, 317 (1992).

[7]The lowest optical-phonon energy in CdSe is 21 meV, giving a negligible optical-phonon population below 50 K.

[8]W. C. Tait and R. L. Weiher, Phys. Rev. **166**, 769 (1968).

[9]N. N. Zinov'ev, L. P. Ivanov, I. G. Lang, S. T. Pavlov, A. V. Prokaznikov, and I. D. Yaroshetskiĭ, Zh. Eksp. Teor. Fiz. **84**, 2153 (1983) [Sov. Phys. JETP **57**, 1254 (1983)].

[10]R. K. Jain and M. B. Klein, in *Optical Phase Conjugation,* edited by R. A. Fischer (Academic, New York, 1983), pp. 307–415.

[11]H. J. Eichler, P. Günter, and D. W. Pohl, *Laser-Induced Dynamic Gratings,* Springer Series in Optical Sciences Vol. 50 (Springer-Verlag, Berlin, 1986).

[12]C. Dörnfeld and J. M. Hvam, IEEE J. Quantum Electron. **QE-25**, 904 (1989).

[13]J. R. Salcedo, A. E. Siegmann, D. Dlott, and M. D. Fayer, Phys. Rev. Lett. **41**, 131 (1978).

[14]Y. Masumoto and S. Shionoya, Phys. Rev. B **30**, 1076 (1984).

[15]V. V. Travnikov and V. V. Krivolapchuk, Pis'ma Zh. Eksp. Teor. Fiz. **34**, 347 (1981) [JETP Lett. **34**, 330 (1981)].

[16]V. V. Travnikov and V. V. Krivolapchuk, Fiz. Tverd. Tela (Leningrad) **24**, 961 (1982) [Sov. Phys. Solid State **24**, 547 (1982)].

[17]Y. Toyozawa, Prog. Theor. Phys. (Kyoto) Suppl. **12**, 111 (1959).

[18]C. Hermann and P. Y. Yu, Phys. Rev. B **21**, 3675 (1980).

[19]I. Broser, R. Broser, and A. Hoffmann, in *Semiconductors,* edited by O. Madelung, Landolt-Börnstein, New Series, Group III, Vol. 17b (Springer-Verlag, Berlin, 1982), pp. 202–224.